

# Dark-bright mixing of interband transitions in symmetric semiconductor quantum dots

G. Sallen<sup>1</sup>, B. Urbaszek<sup>1,\*</sup>, M. M. Glazov<sup>2</sup>, E. L. Ivchenko<sup>2</sup>, T. Kuroda<sup>3</sup>, T. Mano<sup>3</sup>, S. Kunz<sup>1</sup>, M. Abbarchi<sup>3</sup>, K. Sakoda<sup>3</sup>, D. Lagarde<sup>1</sup>, A. Balocchi<sup>1</sup>, X. Marie<sup>1</sup>, and T. Amand<sup>1</sup>  
<sup>1</sup>Université de Toulouse, INSA-CNRS-UPS, LPCNO, 135 Av. Rangueil, 31077 Toulouse, France  
<sup>2</sup>Ioffe Physical-Technical Institute RAS, 194021 St.-Petersburg, Russia and  
<sup>3</sup>National Institute for Material Science, Namiki 1-1, Tsukuba 305-0044, Japan  
(Dated: April 25, 2022)

In photoluminescence spectra of symmetric [111] grown GaAs/AlGaAs quantum dots in longitudinal magnetic fields applied along the growth axis we observe in addition to the expected bright states also nominally dark transitions for both charged and neutral excitons. We uncover a strongly non-monotonous, sign changing field dependence of the bright neutral exciton splitting resulting from the interplay between exchange and Zeeman effects. Our theory shows quantitatively that these surprising experimental results are due to magnetic-field-induced  $\pm 3/2$  heavy-hole mixing, an inherent property of systems with  $C_{3v}$  point-group symmetry.

PACS numbers: 72.25.Fe, 73.21.La, 78.55.Cr, 78.67.Hc  
Keywords: Quantum dots, optical selection rules

The search of methods to generate and manipulate entangled quantum states is one of the driving forces behind experimental physics on the nano-scale. The initial proposal to use the exciton-biexciton cascade in quantum dots to generate entangled photon pairs [1] relies on symmetric dots where the neutral exciton  $X^0$  states are degenerate, i.e. have zero fine structure splitting  $\delta_1$  induced by anisotropic electron-hole Coulomb exchange. As in practice  $\delta_1 \neq 0$  in the majority of quantum dot systems [2–4], very inventive research has been developed trying to tune the fine structure splitting to zero with original techniques [5–8]. An alternative, recent approach is to use samples grown along the  $z' \parallel [111]$  crystallographic axis, which is also the orientation of most nano-wires [9]. This growth axis has the advantage of providing microscopically identical interfaces for quantum well or dot structures, resulting in  $C_{3v}$  point symmetry. Hence, small fine structure splittings in *as grown* [111] quantum dot structures have been recently predicted [10, 11] and observed [12–14] followed by a first report of photon entanglement [15].

In the commonly studied dot samples grown along  $z \parallel [001]$  axis, the exact nature and symmetry of the  $X^0$  and charged exciton states is deduced from experiments in longitudinal magnetic fields i.e. parallel to the growth axis. These studies made crucial contributions to the development of quantum dot photonics and spin physics [3, 4, 16]. Here we study the effect of a longitudinal magnetic field  $\mathbf{B} \parallel z' \parallel [111]$  in strain free [111] grown GaAs quantum dots. In  $B_{z'} \neq 0$  we observe *four* emission lines, as two nominally dark transitions emerge in addition to the usual bright Zeeman doublet for charged excitons and  $X^0$  of all quantum dots investigated. Our measurements show that the heavy hole states with spin

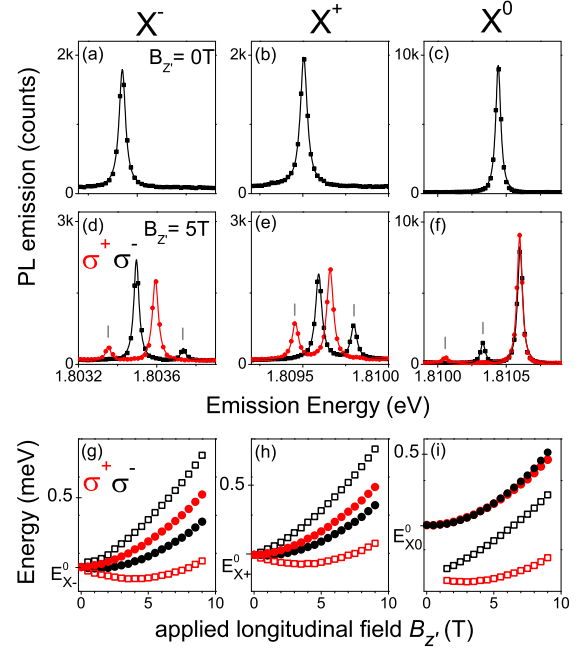


FIG. 1: (Color online): (a)-(c) single dot PL spectra at  $B_{z'} = 0$ . (d)-(f) single dot PL spectra at  $B_{z'} = 5$  T, for  $\sigma^-$  (black line/solid squares) and  $\sigma^+$  (red line/circles) (g)-(i) transition energies as a function of  $B_{z'}$ , for  $\sigma^-$ : dark (black hollow squares) and bright (black circles) and  $\sigma^+$ : (red hollow squares) and bright (red circles). Data are shown for **QD I**.

projections  $+3/2$  or  $-3/2$  onto the growth axis  $z'$  are coupled in a longitudinal magnetic field. The resulting appearance of forbidden charged exciton and dark  $X^0$  transitions due to hole mixing is an inherent feature of [111] grown dots and is not related to a symmetry lowering, of the confinement potential or due to strain, as in [001] grown dots [3, 4]. We are able to measure the dark-bright  $X^0$  separation and observe a strongly non-

\*Corresponding author : urbaszek@insa-toulouse.fr

monotonous bright  $X^0$  splitting that changes sign as a function of  $B_{z'}$  due to the competition between isotropic electron-hole Coulomb exchange and the Zeeman interactions. We explain all these intriguing findings by a microscopic model of the Zeeman interaction accounting for  $C_{3v}$  point symmetry of the studied quantum dots. The key ingredient of our theory is to include the cubic terms for the hole hamiltonian [17, 18] going beyond the commonly used spherical approximation. We extract sign and magnitude of electron and hole  $g$  factors for this new system.

The sample was grown by droplet epitaxy using a conventional molecular beam epitaxy system [12, 19, 20] on a GaAs(111)A substrate. The dots are grown on 100nm thick  $\text{Al}_{0.3}\text{Ga}_{0.7}\text{As}$  barriers and are covered by 50nm of the same material. There is no continuous wetting layer in the sample connecting the dots (typical height  $\simeq 3\text{nm}$ , radius  $\simeq 15\text{nm}$ ), see details in [12]. Single dot photoluminescence (PL) at 4K is recorded with a home build confocal microscope with a detection spot diameter of  $\simeq 1\mu\text{m}$ . The detected PL polarization is analysed and the signal is dispersed by a spectrometer and detected by a Si-CCD camera. Optical excitation is achieved by pumping the AlGaAs barrier with a HeNe laser at 1.96 eV that is linearly polarized to exclude the effects of optical carrier orientation and dynamic nuclear polarization [21].

Figure 1a-c shows the different emission lines originating from a typical quantum dot QD I at zero magnetic field. The  $X^0$ , the negatively charged exciton  $X^-$  (2 electrons, 1 hole) and the positively charged exciton  $X^+$  (1 electron, 2 holes) are identified using fine structure analysis and optical orientation experiments [21]. The high symmetry of the dots is reflected in typical values for the splitting of the  $X^0$  emission due to anisotropic electron-hole exchange  $\delta_1$  of a few  $\mu\text{eV}$  [12], extracted from angle dependent PL polarization analysis in the linear basis.

In figure 1d-f the  $\sigma^+$  and  $\sigma^-$  polarized emission from the same exciton states are presented in the presence of a longitudinal magnetic field  $B_{z'} = 5\text{T}$ . We first discuss charged excitons  $X^+$  and  $X^-$ , whose emission energies are shown in Fig. 1g,h. In contrast to the widely studied [001] grown samples, where a Zeeman doublet is observed, with one  $\sigma^+$  and one  $\sigma^-$  polarized branch [3, 19, 20, 22] here the emission patterns are strikingly different: We observe in total four transitions, two of them are  $\sigma^+$  polarized, and two others are  $\sigma^-$  polarized. For each polarization, the more intense emission line will be called "bright", the less intense "dark" in the following. The emission of two doublets is observed for the  $X^+$  and the  $X^-$  exciton of all the dots studied as soon as  $|B_{z'}| > 0$  in this sample, see Fig. 1g,h. The measured ratio of the emission intensity bright /dark transitions remains constant as  $|B_{z'}|$  changes (not shown).

We also note the appearance of dark states for the  $X^0$  emission in Fig. 1f,i. For typically  $|B_{z'}| > 2\text{T}$  we are able to detect that the bright  $X^0$  emission is accompanied by less intense lines at  $\delta_0 \simeq 350\mu\text{eV}$  lower in energy. This energy separation  $\delta_0$  is due to isotropic electron-

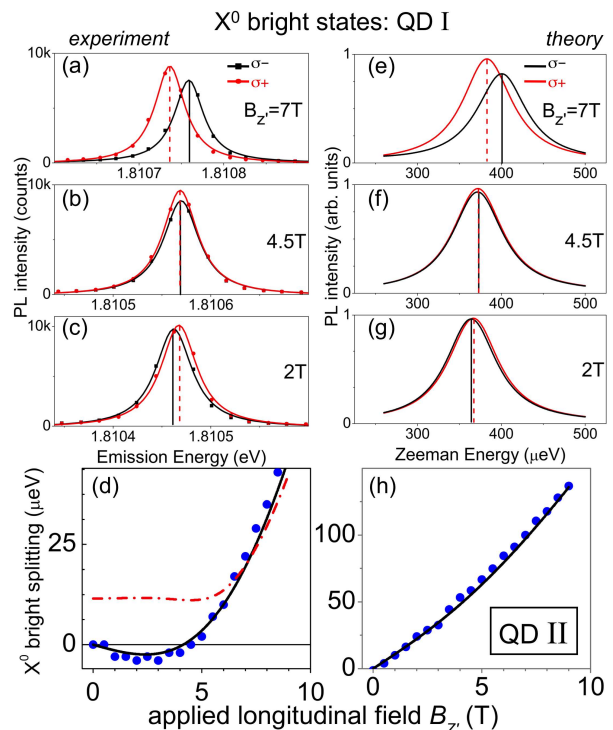


FIG. 2: (Color online): (a)-(c) PL spectra in  $\sigma^{+/-}$  polarizations of bright  $X^0$  for different  $B_{z'}$ . (d) bright  $X^0$  Zeeman splitting  $E(\sigma^-) - E(\sigma^+)$  vs  $B_{z'}$ : experiment (circles), theory (black line), theoretical value of total splitting including  $\delta_1 = 11\mu\text{eV}$  (dotted red line); (e)-(g) calculated spectra. Panels (a)-(g) correspond to **QD I**. (h) as (d) but for **QD II**.

hole exchange which splits bright and dark states. Previously, dark  $X^0$  states have been observed generally for dots grown along the [001] axis either in high *transverse* magnetic fields (Voigt geometry) [23] or exceptionally in high *longitudinal* magnetic fields for dots with lowered symmetry [3, 22]. In the dots grown along [111] investigated here the dark  $X^0$  is clearly visible for *all* dots in this sample in the Faraday configuration, even for highly symmetric dots with vanishing  $\delta_1$ .

Another surprising feature of the  $X^0$  emission is shown in Fig. 1i and analyzed in detail in Fig. 2a-c. At 2T, the  $\sigma^+$  polarized branch is at *higher* energy, at 4.5T both  $\sigma^+$  and  $\sigma^-$  emission coincide in energy and at  $B_{z'} > 4.5\text{T}$  the  $\sigma^+$  is finally at *lower* energy. So the Zeeman splitting versus  $B_{z'}$  is first tending towards negative values, before decreasing in amplitude to pass through zero at  $B_{z'}^0 \simeq 4.5\text{T}$  to finally become positive. For dots showing this reversal in sign for the Zeeman splitting, the exact value of  $B_{z'}^0$  varies from dot to dot. The Zeeman splitting extracted from the spectra following the procedure of Ref. [21] is plotted in Fig. 2d and clearly demonstrates the change in sign.

The evolution of the bright  $X^0$  splitting varies dramatically from dot to dot: For QD II which has at  $B_{z'} = 0$  very similar emission characteristics to QD I (transition energy, exciton states, values of  $g$  factors and exchange

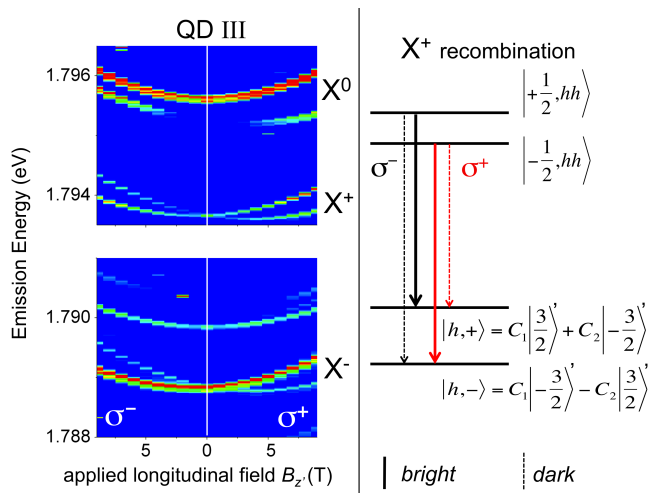


FIG. 3: (Color online) Left: Bright and dark states for **QD III** vs  $B_{z'}$ . Right: Scheme of recombination of  $X^+$  with mixed hole states, see Eq. 1.

energies) we record a splitting that is always positive and does not change sign, see Fig. 2h. The absolute value of the Zeeman splitting at  $B_{z'} = 9$  Tesla is a factor of three higher in QD II than in QD I. Both dots QD I and QD II show prominent dark state emission and for both dots the dark state Zeeman splitting is a monotonous function of  $B_{z'}$ , as shown in Fig. 1i for QD I.

At the origin of all these surprising effects lies the magnetic field induced mixing between the heavy hole states with the angular momentum projection  $\pm 3/2$  onto the growth axis  $z'$ . Let us introduce the coordinate system  $x' \parallel [11\bar{2}]$ ,  $y' \parallel [\bar{1}10]$  and  $z' \parallel [111]$  relevant for the structure under study and the heavy-hole basis functions  $|3/2\rangle', |-3/2\rangle'$  which transform according to the representation  $\Gamma_5 + \Gamma_6$ , where  $\Gamma_{5,6}$  are irreducible representations of the group  $C_{3v}$ . It is crucial to note that the symmetry properties of the field  $B_{z'}$  are described by the representation  $\Gamma_2$  and the direct product  $(\Gamma_5 + \Gamma_6) \times (\Gamma_5^* + \Gamma_6^*) = 2\Gamma_1 + 2\Gamma_2$  contains not one, but two representations  $\Gamma_2$ . As a result the heavy-hole Zeeman splitting in the basis  $|3/2\rangle', |-3/2\rangle'$  is described by the  $2 \times 2$  matrix with two linearly independent coefficients

$$\mathcal{H}_B = \frac{1}{2} \mu_B B_{z'} \begin{bmatrix} g_{h1} & g_{h2} \\ g_{h2} & -g_{h1} \end{bmatrix}. \quad (1)$$

Here  $\mu_B$  is the Bohr magneton,  $g_{h1}$  and  $g_{h2}$  are the effective hole  $g$ -factors. We emphasize that the above arguments hold for heavy holes in a system of any dimensionality  $nD$  ( $n = 0 \dots 3$ ) provided its symmetry is trigonal, including an exciton formed in bulk Germanium by an electron in the  $L$ -valley and a  $\Gamma_8^+$  hole. [24] In contrast, in conventional [001] grown structures, the longitudinal-field induced mixing of heavy holes is symmetry-forbidden,  $g_{h2} \equiv 0$  [25]. Microscopically, a non-zero value of the off-diagonal coefficient  $g_{h2}$  in the [111] grown systems can already be obtained within the framework of the bulk hole Zeeman Hamiltonian which in the cubic axes  $x, y, z$  reads [17]

$$\mathcal{H}_B = -2\mu_B [\kappa \mathbf{J} \cdot \mathbf{B} + q(J_x^3 B_x + J_y^3 B_y + J_z^3 B_z)], \quad (2)$$

where  $\kappa$  and  $q$  are dimensionless coefficients,  $J_x, J_y$  and  $J_z$  are the angular momentum matrices in the  $\Gamma_8$  basis. Transition in Eq. (2) to the coordinate system  $x', y', z'$  gives the relations between the pairs of coefficients in Eqs. (1) and (2):  $g_{h1} = -[6\kappa + (23/2)q]$ ,  $g_{h2} = 2\sqrt{2}q$ . In bulk semiconductors the coefficient  $q$  is too small [18] to be responsible for high values of  $g_{h2}$ . However, in low-dimensional systems the hole  $g$  factors are very sensitive to the strength and shape of the confining potential. Particularly, an important contribution to  $g_{h2}$  could be given by valence-band spin-orbit terms cubic in wave vector  $k$ . The relevant contribution  $\propto J_x^3 k_x (k_y^2 - k_z^2) + \dots$  to the hole Hamiltonian [26] can be recast as  $\mathcal{H}_{v3} = \mathcal{A}^{(3)} (J_{x'}^3 - 3\{J_{x'} J_{y'}^2\}) \text{Im}(k_{x'} - ik_{y'})^3$  where the curly brackets mean the anticommutator [17]. Replacing  $\mathbf{k}$  by  $\mathbf{k} - (e\mathbf{A}/c\hbar)$  with  $\mathbf{A}$  being the vector potential of the magnetic field we obtain

$$g_{h2} = -18 \frac{m_0 \mathcal{A}^{(3)}}{\hbar^2} \left\langle \left( \frac{\partial}{\partial x'} - i \frac{\partial}{\partial y'} \right)^2 (x' - iy') \right\rangle, \quad (3)$$

where  $m_0$  is the free electron mass and the averaging is carried out over the confined-hole envelope function.

In a longitudinal magnetic field, the hole eigen energies are  $E_{\pm} = \pm g_h \mu_B B_{z'}/2$  with  $g_h = \sqrt{g_{h1}^2 + g_{h2}^2}$  and the hole eigenstates  $|h, \pm\rangle$  are admixtures of  $|3/2\rangle'$  and  $|-3/2\rangle'$ , as indicated in Fig. 3, with the coefficients  $C_{1,2}$  determined solely by the ratio  $g_{h2}/g_{h1}$ . For non-zero  $g_{h2}$ , all the four radiative transitions are allowed, each transition being circularly polarized, either  $\sigma^+$  or  $\sigma^-$  [27]. For illustration, the four channels of radiative recombination of a positively charged trion are shown on the right-hand side of Fig. 3, together with the corresponding sign of circular polarization. The transition energies are determined by combinations of the electron and hole effective  $g$ -factors which allows to find a pair of parameters,  $g_e$  and  $g_h = \sqrt{g_{h1}^2 + g_{h2}^2}$ . The intensities of circularly-polarized lines are proportional to  $|C_1|^2$  and  $|C_2|^2$  and independent of the magnetic field, in full agreement with our experiments. From the ratio of intensities of identically-polarized lines we can find the ratio  $g_{h1}/g_h$  and, therefore, determine values of  $g_e$ ,  $g_{h1}$  and modulus of  $g_{h2}$ .

The values of the  $g$  factors vary from dot to dot and even for different complexes  $X^0, X^+, X^-$  in the same dot revealing the importance of confinement and Coulomb interaction for the  $g$ -factor renormalization. Values for five typical dots are listed in Table I [28]. The experimental observation of dark states for all dots investigated leads logically to  $g_{h2} \neq 0$  for all dots.

Dark transition related to  $X^+$  and  $X^-$  complexes are always present in the spectra for all non-zero values of the field. By contrast, emission intensities of dark  $X^0$  states increase gradually with  $B_{z'}$ . This is a result of the effect of electron-hole exchange interaction. Taking into account isotropic short-range and long-range exchange interaction and assuming that the confining potential possesses 3-fold rotation axis we obtain for the  $X^0$  sublevel

TABLE I:  $g$ -factors (typ. error  $\leq 10\%$ ) for charged and neutral excitons obtained from fitting the data. For the  $X^0$  the  $g_e$  and  $g_h$  values obtained for  $X^+$  for the same dot are taken and only  $|g_{h2}|$  is varied to fit the bright and dark  $X^0$  splitting *simultaneously*.

	QD I	QD II	QD III	QD IV	QD V
$X^- : g_e$	0.49	0.46	0.47	0.48	0.50
$g_h$	0.83	0.71	0.81	0.79	0.74
$ g_{h2} $	0.53	0.60	0.53	0.57	0.57
$X^+ : g_e$	0.47	0.44	0.44	0.47	0.50
$g_h$	0.71	0.72	0.72	0.72	0.73
$ g_{h2} $	0.62	0.72	0.68	0.70	0.72
$X^0 :  g_{h2} $	0.50	0.68	0.56	0.59	0.65
$g_e$ and $g_h$ : same values as for $X^+$					

energies

$$E_{s,m} = sg_e\mu_B B_{z'} + \frac{1}{2}(\delta_0 + m\delta_m), \quad (4)$$

$$\delta_m = \sqrt{\delta_0^2 + (g_h\mu_B B_{z'})^2 - 4sg_{h1}\mu_B B_{z'}\delta_0}.$$

Hereafter we assume the exchange splitting between bright and dark states,  $\delta_0 > 0$ ,  $s = \pm 1/2$  denotes electron spin,  $m = \pm 1$  denote heavy hole states  $|h, \pm\rangle$ , respectively. At zero magnetic field the higher sublevels ( $\pm 1/2, +$ ) are bright and the lower sublevels ( $\pm 1/2, -$ ) are forbidden. The optical activity of the dark states is induced by the magnetic field in our experiments [29]. Exciton energy is referred to the zero-field dark state with  $m = -1$ . It follows from Eq. (4) that the splitting of bright  $X^0$  states,  $E_{+1/2,+}(B_{z'}) - E_{-1/2,+}(B_{z'})$ , can be a non-monotonous and sign-changing function of  $B_{z'}$ . This is confirmed by our measurements shown in Fig. 2d, where the calculation (solid line) follows closely the experiment (dots). The most surprising feature, the vanishing  $X^0$  splitting at  $B_{z'} = B_{z'}^0$  is well reproduced by the model. This result is another striking difference when comparing with the work on [001] grown dots, where the observed splitting increases monotonously as a function of the applied longitudinal field [3, 4, 22]. The fit of

the data in Fig. 2d is very sensitive to the exact value of  $|g_{h2}|$  which explains the strong variations of the  $X^0$  bright splittings as a function of  $B_{z'}$  from dot to dot. To go from the strongly non-monotonous behavior for QD I to the more monotonous graph for QD II in Fig. 2h, a change of  $|g_{h2}|$  of only about 20% is sufficient, all other parameters remaining constant. Here the development of a microscopic theory for  $g_{h1}$  and  $g_{h2}$  for realistic quantum dot samples will deepen our understanding.

Taking into account (i) the energy dependence of the bright  $X^0$  on  $B_{z'}$ , (ii) the polarization of the  $X^0$  eigenstates and our spectral resolution we calculate the emission spectra in the  $\sigma^+/\sigma^-$  basis using the fitted  $g$ -factor values. Our theory shown in Fig. 2e-g reproduces the measurements very accurately in terms of sign and value of the splitting and emission polarization. Interestingly, the  $X^0$  eigenstates 'exchange' polarization at the field value  $B_{z'}^0$ . For  $B_{z'} < B_{z'}^0$ , the calculations and measurements show that the higher lying state is  $\sigma^+$  polarized and the lower  $\sigma^-$ ; at  $B_{z'} > B_{z'}^0$ , it is the opposite. Inclusion of small but non-zero anisotropic splitting of bright doublet,  $\delta_1$ , results in the non-vanishing splitting of the eigenstates for all values of  $B_{z'}$ , as shown in Fig. 2d by the dash-dotted curve. However, at  $B_{z'} \approx 0$  and  $B_{z'}^0$ ,  $\sigma^+$  and  $\sigma^-$  polarized lines exchange their places. Our measurement scheme allows us to extract the Zeeman splitting only [21]. The influence of  $\delta_1$  and the determination of exact polarization eigenstates of the system sets the challenge for future experiments, aiming to eventually tune the  $X^0$  splitting to zero to erase the 'which path' information, a necessary condition for the generation of entangled photon pairs from the biexciton-exciton cascade [5, 6]. Also additional energy shifts due to nuclear spin effects will be explored in this context. Traces of heavy-hole mixing should also be investigated in [111] grown GaAs/AlGaAs quantum wells [30], currently at the centre of interest due to the predicted ultra-long electron spin relaxation times [31].

We thank ANR QUAMOS, ANR SPINMAN, ITN SPINOPTRONICS, RFBR, LIA CNRS ILNACS and Dynasty Foundation for support.

- 
- [1] O. Benson et al., Phys. Rev. Lett. **84**, 2513 (2000).
  - [2] D. Gammon et al., Phys. Rev. Lett. **76**, 3005 (1996).
  - [3] M. Bayer et al., Phys. Rev. Lett. **82**, 1748 (1999).
  - [4] L. Besombes et al., Phys. Rev. Lett. **85**, 425 (2000).
  - [5] R. M. Stevenson et al., Nature (London) **439**, 179 (2006).
  - [6] J. D. Plumhof et al., Phys. Rev. B **83**, 121302 (2011).
  - [7] W. Langbein et al., Phys. Rev. B **69**, 161301 (2004).
  - [8] N. Akopian et al., Phys. Rev. Lett. **96**, 130501 (2006).
  - [9] W. Lu and C. M. Lieber, J. of Physics D **39**, R387 (2006).
  - [10] A. Schliwa et al., Phys. Rev. B **80**, 161307 (2009).
  - [11] R. Singh and G. Bester, Phys. Rev. Lett. **103**, 063601 (2009).
  - [12] T. Mano et al., Appl. Phys. Express **3**, 065203 (2010).
  - [13] K. F. Karlsson et al., Phys. Rev. B **81**, 161307 (2010).
  - [14] E. Stock et al., Appl. Phys. Lett. **96**, 093112 (2010).
  - [15] A. Mohan et al., Nat. Photon. **4**, 302 (2010).
  - [16] M. Paillard et al., Phys. Rev. Lett. **86**, 1634 (2001).
  - [17] *Superlattices and Other Heterostructures*, E.L. Ivchenko and G. Pikus, Springer Series in Solid-State Sciences, Berlin 1995.
  - [18] X. Marie et al., Phys. Rev. B **60**, 5811 (1999).
  - [19] M. Abbarchi et al., Phys. Rev. B **81**, 035334 (2010).
  - [20] T. Belhadj et al., Phys. Rev. B **78**, 205325 (2008).
  - [21] T. Belhadj et al., Phys. Rev. Lett. **103**, 086601 (2009).
  - [22] Y. Léger et al., Phys. Rev. B **76**, 045331 (2007).
  - [23] J. Puls et al., Phys. Rev. B **60**, R16303 (1999).
  - [24] N. S. Averkiev et al., Sov. Phys. Solid State **23**, 1851 (1981).

- [25] A symmetry analysis for a transverse magnetic field in the plane of (111) grown dots predicts in first order no mixing of the  $|3/2\rangle'$  and  $|-3/2\rangle'$  states.
- [26] E. I. Rashba and E. Y. Sherman, Phys. Lett. A **129**, 175 (1988).
- [27] If in addition to the discussed effects heavy-hole to light-hole coupling were important, four lines would be observed for both  $\sigma^+$  and  $\sigma^-$  polarized emission.
- [28] In bulk GaAs  $g_e = -0.44$  and for AlGaAs  $g_e = 0.5$ .  $g_e$  evolves monotonously towards the barrier material for GaAs/AlGaAs quantum wells of decreasing thickness [17]. These results, together with the fact that  $|g_e| > 0.44$  in most cases confirm that  $g_e$  is positive.
- [29] The short-range anisotropic cubic exchange interaction  $\propto \sigma_x J_x^3 + \sigma_y J_y^3 + \sigma_z J_z^3$  can mix bright and dark  $X^0$  states. Our measurements show that its effect is negligible since no dark  $X^0$  state emission is detected at  $B_{z'} = 0$ . So the cubic exchange term can be neglected in our [111] grown dots, which helps clarifying differences between previous predictions of the nature of the  $X^0$  emission [10, 11, 13].
- [30] L. Viña et al., Phys. Rev. B **46**, 13234 (1992).
- [31] X. Cartoixà et al., Phys. Rev. B **71**, 045313 (2005).